Journal of The Electrochemical Society

OPEN ACCESS

Thermodynamic Properties of Ni–Dy Intermetallic Compounds Measured Electrochemically in Molten $CaCl_2$–$DyCl_3$

To cite this article: Hang Hua *et al* 2021 *J. Electrochem. Soc.* **168** 102501

Journal of The Electrochemical Society, 2021 **168** 102501

Thermodynamic Properties of Ni–Dy Intermetallic Compounds Measured Electrochemically in Molten $CaCl_2$–$DyCl_3$

Hang Hua,[1] Kouji Yasuda,[2,*] and Toshiyuki Nohira[1,*,z]

[1]*Institute of Advanced Energy, Kyoto University, Gokasho, Uji, Kyoto 611-0011, Japan*
[2]*Graduate School of Engineering, Kyoto University, Yoshida-honmachi, Sakyo-ku, Kyoto 606-8501, Japan*

The temperature dependence of the coexisting phase potentials of various Nickel–Dysprosium (Ni–Dy) intermetallic compounds in a molten $CaCl_2$–$DyCl_3$ (1.0 mol% added) system was determined between 1073 K and 1173 K at 25 K intervals. The coexisting phase potentials of (NiDy + Ni_2Dy), (Ni_2Dy + Ni_3Dy), (Ni_3Dy + Ni_5Dy), and (Ni_5Dy + Ni) were measured via open-circuit potentiometry using a Ni flag electrode. The Dy activities and the Dy relative partial molar Gibbs energies in Ni–Dy intermetallic compounds were calculated from these potentials. Then, the Ni activities and the Ni relative partial molar Gibbs energies were calculated using the Gibbs-Duhem equation. Thereafter, the relative partial molar enthalpies and entropies of Dy and Ni were obtained by comparing the temperature dependence equations of the relative partial molar Gibbs energies. Finally, the relative partial molar Gibbs energies of Dy and Ni were used to calculate the standard Gibbs energies of formation for various Ni–Dy intermetallic compounds and compared with reported values.

 [DOI: 10.1149/1945-7111/ac2beb]

Manuscript submitted August 10, 2021; revised manuscript received September 27, 2021. Published October 12, 2021.

Rare earth (RE) elements have been the focus of studies over the past fifty years because they have unique properties when alloyed with other elements. For example, the magnetic properties of Nd–Fe–B[1–3] and Sm–Co,[4] the magnetostrictive properties of Tb–Fe,[5] the hydrogen storage abilities of Ni–RE,[6–8] and the catalytic properties of Pt–RE and La–Fe–O[9,10] are employed in typical applications of REs. Among these remarkable properties, the magnetism of Nd–Fe–B ($Nd_2Fe_{14}B$) has attracted a great deal of attention in recent years because of the widespread use of battery electric vehicles (BEVs) and hybrid electric vehicles (HEVs). The $Nd_2Fe_{14}B$ magnet, which is the strongest permanent magnet commercially available, displays the highest maximum energy product of 470 kJ m^{-3}.[11] In addition to superior magnetic properties, the $Nd_2Fe_{14}B$ magnet has the advantages of a high mechanical strength and a reasonable production cost. Almost the only drawback of the $Nd_2Fe_{14}B$ magnet is its low Curie temperature of 585 K.[12] These properties meet all the performance requirements for magnets used in the high-performance motors of BEVs and HEVs except for the low Curie temperature. To maintain superior magnetic properties during the high temperature operation of motors, the addition of Dy to the magnet is necessary.[13] From the viewpoint of global environmental issues, the production of environmentally friendly BEVs and HEVs is expected to increase dramatically and the demand for Nd and Dy will simultaneously increase. However, Nd and Dy are produced together with other rare earths, but their content in the ore is not high. Furthermore, due to the cost and environmental challenges associated with their extraction and selective separation and reduction, their supply in the market is under tension. Another problem is the particularly unstable supply of Dy due to its uneven distribution in China. Thus, the recycling of REs from scrap magnets is a feasible method to ensure supply security in countries with scarce RE resources. In addition, the production of electronic product waste (e-waste) containing REs, such as fluorescent lamps, has been increasing rapidly recently,[14] however, it has not yet reached the level of industrial recycling. Currently, on-site recycling of waste is partly carried out at manufacturing plants of Nd magnets, using a combination of wet leaching and solvent extraction methods.[15] However, disadvantages such as high energy utilization, multistep processes, and high environmental load prevent the further development of conventional RE recycling processes.

Several pyrometallurgical methods have been proposed as new RE recovery processes. Adachi et al. proposed a recycling method named chemical vapor transport (CVT), here they applied the vapor pressure difference of RE salts at high temperatures to separate RE elements in the form of gas complexes.[16] Uda et al. reported a separation process for REs involving the vacuum distillation of dihalide and trihalide mixtures.[17] The principle was similar to that of the CVT method, i.e., they applied the vapor pressure difference between $RECl_2$/$RECl_3$ and REI_2/REI_3. Although these two methods involved simpler processes with fewer steps than hydrometallurgical processes, they failed to achieve a high ratio of separation between each RE element. Meanwhile, several processes based on the selective extraction of REs from scrap magnets have been proposed.[18–26] Molten Mg, $MgCl_2$, Ag, NH_4Cl, $FeCl_2$, and B_2O_3 were applied as the extraction agents in these processes. Although a good separation between REs and other elements was achieved, the separation of the individual RE elements was not the focus of their studies.

We proposed a method for the efficient separation and recovery of REs by selective electrochemical formation of Ni–RE intermetallic compounds in molten salt.[27–29] We have demonstrated the formation of Ni–Nd and Ni–Dy intermetallic compounds and the separation of Dy/Nd in molten LiF–CaF_2 at 1123 K,[27] in NaCl–KCl at 973 K,[28] and in LiCl–KCl at approximately 700 K.[29] Previous studies have shown that high formation rates of Ni–RE intermetallic compounds were obtained when operating at high temperatures. For example, the Ni–RE intermetallic compound formation rate was over 200 μm h^{-1} at 1123 K.[27] High separation ratios can be obtained in chloride systems, e.g., a Dy was enriched 72-fold against Nd in LiCl–KCl system.[29] Therefore, we aimed to develop a chloride melt that can operate at high temperatures for the achievement of both high alloy formation rate and high Dy/Nd separation ratio.

Recently, the calcium chloride ($CaCl_2$) system has received much attention as it enables operation at high temperatures with low vapor pressure. Firstly, the electrolytic formation of Ni–Dy and Ni–Nd intermetallic compounds in molten $CaCl_2$–$DyCl_3$ and $CaCl_2$–$NdCl_3$ at 1123 K, respectively, were investigated.[30,31] For Ni–Dy system, we have already reported that the potentials of the coexisting (NiDy + Ni_2Dy), (Ni_2Dy + Ni_3Dy), (Ni_3Dy + Ni_5Dy), and (Ni_5Dy + Ni) phases at 1123 K.[30] From the coexisting phase potentials, the standard Gibbs energies of formation for Ni–Dy intermetallic compounds were calculated. To further understand other thermodynamic quantities of Ni–Dy intermetallic compounds, such as the standard enthalpies and entropies of formation, data collection on the

*Electrochemistry Society Member.
[z]E-mail: nohira.toshiyuki.8r@kyoto-u.ac.jp

temperature dependence is required. Several researchers have reported the thermodynamic quantities of Ni–Dy intermetallic compounds determined by different methods. Konishi et al. reported the thermodynamic quantities in molten LiCl–KCl between 673 K and 773 K.[32] The relative partial molar thermodynamic properties, activities of Dy and Ni, and the standard Gibbs energies of formation for the Ni–Dy intermetallic compounds were calculated. Li et al. reported the thermodynamic quantities of the Ni–Dy system generated via CALPHAD technique[33] based on experimental data.[34] The standard enthalpies and Gibbs energies of formation for the Ni–Dy intermetallic compounds, as well as the activities of Ni and Dy were calculated. Except for the above two systematic reports, Schott and Sommer measured the standard enthalpies of formation for $NiDy_3$, NiDy, Ni_2Dy, and Ni_5Dy at 1098 K[35] and Guo et al. described the standard enthalpies of formation for NiDy and Ni_5Dy at 1474 K.[36] However, between 1073–1173 K, the target temperature range of appliable to RE recycling, no systematic experimental data have been generated. In this study, the temperature dependence of coexisting phase potentials for the Ni–Dy intermetallic compounds were systematically measured to obtain the thermodynamic quantities in the temperature range of 1073–1173 K at 25 K intervals in molten $CaCl_2$.

Experimental

The electrolysis setup is shown in Fig. 1. Three hundred grams of $CaCl_2$ (purity: 99.9%) obtained from Kojundo Chemical Laboratory Co. Ltd., was introduced in a graphite crucible (IG-110, Toyo Tanso Co. Ltd., i.d.: Φ 90 mm, h.: 120 mm). They were placed in a vacuum oven for more than 72 h at 453 K for preliminary drying. The crucible was then placed at the bottom of a stainless-steel chamber in a Kanthal airtight container for further drying under vacuum at 773 K for 24 h in an argon (Ar) atmosphere glove box. After the drying, the Kanthal container was replenished with Ar gas until atmospheric pressure was reached, while the temperature was increased to 1073 K. When the temperature of salt stabilized at 1073 K, anhydrous $DyCl_3$ (purity: 99.9%) obtained from Kojundo Chemical Laboratory Co. Ltd, was directly added into the melt at a concentration of 1.0 mol% as Dy^{3+} ion source. A Mo flag (>99%, Nilaco Corp., d.: Φ 3.0 mm, t.: 0.1 mm, lead wire d.: Φ 0.2 mm), a Ni flag (>99%, Nilaco Corp.), and a Dy rod (>99.9%, Nilaco Corp., d: Φ 6.35 mm, l.: 50 mm) were used as working electrodes for the electrochemical measurements. A carbon rod (Toyo Tanso Co. Ltd., d.: Φ7 mm, l.: 520 mm) was used as the counter electrode. A Ni wire immersed in molten $CaCl_2$ containing 1.0 mol% $NiCl_2$ (98%, Alfa Aesar Corp.) set in a mullite tube (HB grade, Nikkato Corp., o.d.: Φ 6 mm, i.d.: Φ 4 mm, l.: 500 mm) was used as the reference electrode. Initially, the potential of the reference electrode was calibrated in reference to the Ca^{2+}/Ca potential via cyclic voltammetry. The potential of Dy^{3+}/Dy was measured via open-circuit potentiometry after immersing the Dy rod in molten salt. After potentiostatic electrolysis at a Ni electrode, open-circuit potentiometry was performed to determine the coexisting phase potentials of the Ni–Dy intermetallic compounds. In order to determine the thermodynamic quantities, the potentials were stated in reference to the Dy^{3+}/Dy potential for further calculation. All the measurements were carried out with an electrochemical workstation (HZ-7000, Hokuto Denko Corp.). The same measurements were conducted at 1073, 1098, 1123, 1148, and 1173 K to determine the temperature dependence of the coexisting phase potentials.

Results and Discussion

The Ni–Dy phase diagram[37] indicates that 9 intermetallic compounds (Ni_2Dy_3, NiDy, Ni_2Dy, Ni_3Dy, Ni_7Dy_2, Ni_4Dy, $Ni_{17}Dy_4$, Ni_5Dy, and $Ni_{17}Dy_2$) and a liquid alloy may exist in the experimental temperature range of 1073–1173 K. In our previous study,[30] only NiDy, Ni_2Dy, Ni_3Dy, and Ni_5Dy were experimentally confirmed via X-ray diffraction (XRD) together with energy-dispersive X-ray spectroscopy (EDX) in molten $CaCl_2$ system at

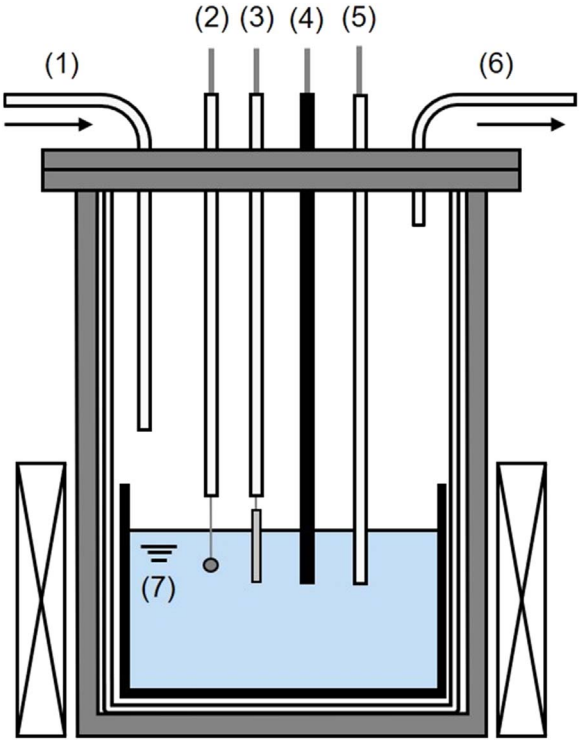

Figure 1. Schematic drawing of the experimental apparatus for the molten $CaCl_2$–$DyCl_3$ system. (1) Ar gas inlet, (2) working electrode (Mo or Ni flag), (3) working electrode (Dy rod), (4) counter electrode (carbon rod), (5) reference electrode (Ni^{2+}/Ni), (6) gas outlet, and (7) $CaCl_2$ molten salt (1.0 mol% $DyCl_3$ included).

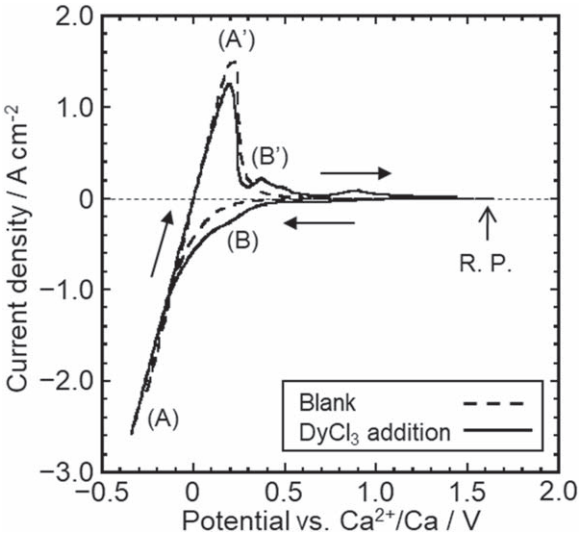

Figure 2. Cyclic voltammograms for a Mo flag electrode in the molten $CaCl_2$ system before and after the addition of 1.0 mol% $DyCl_3$ at 1073 K. Scan rate: 100 mV s^{-1}.

1123 K. Since several Ni–Dy intermetallic compounds were not confirmed for this system, further evaluations of the system were conducted based only on the metastable states. The coexisting phase potentials were determined via open-circuit potentiometry at 1123 K. However, the temperature dependence for the coexisting phase potentials has not been investigated yet.

In the present study, the coexisting phase potentials were measured at various temperatures (1073, 1098, 1123, 1148, and 1173 K) as follows: First, cyclic voltammetry was conducted using a

Mo electrode and the reversal potential was set at a sufficiently negative value (approximately −0.3 V vs Ca^{2+}/Ca) for measuring the deposition/dissolution potential of Ca. Figure 2 shows typical cyclic voltammogram obtained at a Mo electrode after the addition of 1.0 mol% $DyCl_3$ to the $CaCl_2$ system at 1073 K. For comparison, the voltammogram measured before the addition of $DyCl_3$ is also shown in Fig. 2. In both cyclic voltammograms, a pair of rapid cathodic and anodic currents, (A)/(A′), were observed at 0 V. Since Mo does not alloy with Ca between 1073 and 1173 K, (A)/(A′) correspond to the electrodeposition and dissolution of Ca metal. The intersectional potential of the anodic sweep line and the 0 A cm^{-2} line represent the Ca^{2+}/Ca potential. Compared with the blank measurement, larger cathodic and anodic currents, (B)/(B′), were confirmed at approximately 0.3 V for the melt after the addition of $DyCl_3$. Since no Dy–Mo intermetallic compounds exist between 1073 and 1173 K, (B)/(B′) should correspond to the electrodeposition/dissolution of Dy metal.

Then, in order to accurately measure the coexisting phase potentials of Ni–Dy intermetallic compounds, open-circuit potentiometry was performed at a Ni flag electrode at (a) 1073, (b) 1098, (c) 1123, (d) 1148, and (e) 1173 K in molten $CaCl_2$–$DyCl_3$. The obtained potentiograms are shown as red curves in Fig. 3. After potentiostatic electrolysis at 0.40 V for 20 min, the electrode potential gradually shifted to a more positive value as Dy in the formed Ni–Dy intermetallic compounds diffused into the bulk electrode or dissolved into the melt. The potential simultaneously shifted to positive values when only one Ni–Dy intermetallic compound existed on the electrode surface. On the other hand, potential plateaus were observed when two-phases coexisted on the electrode surface. By extending the positive shift line and the later plateau line, the intersection of these two lines was considered to be the plateau potential in this study. Four potential plateaus appeared and they should correspond to the two-phase coexisting states of (NiDy + Ni_2Dy), (Ni_2Dy + Ni_3Dy), (Ni_3Dy + Ni_5Dy), and (Ni_5Dy + Ni) based on our previous study in which XRD measurements of Ni–Dy intermetallic compounds at various potentials were conducted.[30] To measure the equilibrium potential of Dy^{3+}/Dy, a Dy rod electrode was immersed into the melt at each temperature. As shown with blue lines in Fig. 3, a very stable potential was observed at each temperature, which should correspond to the equilibrium potential of Dy^{3+}/Dy. The coexisting phase potentials expressed in reference to the Dy^{3+}/Dy potential at each temperature are shown in Table I, while the regression lines representing the temperature dependences of the coexisting phase potentials are plotted in Fig. 4. The coexisting phase potentials (vs Dy^{3+}/Dy E/V) can be expressed by the following equations:

$$E_{(i)} = 0.350 - 1.73 \times 10^{-4} T\,(\mathrm{NiDy} + \mathrm{Ni_2Dy}) \quad [1]$$

$$E_{(ii)} = 0.358 - 8.04 \times 10^{-5} T\,(\mathrm{Ni_2Dy} + \mathrm{Ni_3Dy}) \quad [2]$$

$$E_{(iii)} = 0.847 - 3.18 \times 10^{-4} T\,(\mathrm{Ni_3Dy} + \mathrm{Ni_5Dy}) \quad [3]$$

$$E_{(iv)} = 0.582 + 7.68 \times 10^{-5} T\,(\mathrm{Ni_5Dy} + \mathrm{Ni}) \quad [4]$$

Based on the temperature dependences of the coexisting phase potentials, the thermodynamic data were calculated. First, the relative partial molar Gibbs energies of Dy ($\Delta\bar{G}_{\mathrm{Dy}}$) and the activities of Dy (a_{Dy}) according to Raoult's law were calculated from E using the following equations,

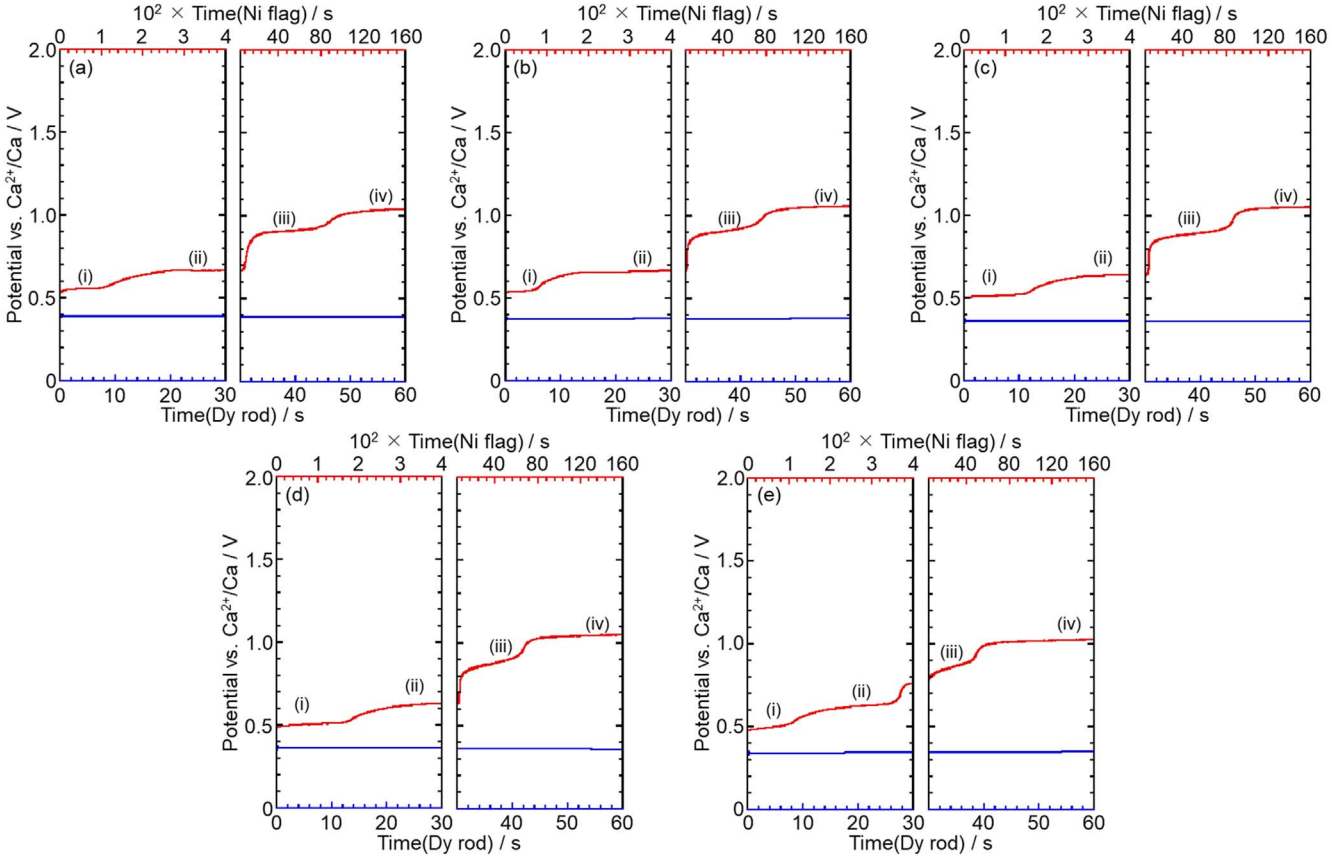

Figure 3. Open-circuit potentiograms for a Ni flag electrode (red curves) after potentiostatic electrolysis at 0.40 V for 20 min and a Dy rod electrode (blue lines) immersed in the molten $CaCl_2$–$DyCl_3$ (1.0 mol%) system at (a) 1073 K, (b) 1098 K, (c) 1123 K, (d) 1148 K, and (e) 1173 K.

Table I. Coexisting phase potentials changes at various temperatures in the molten $CaCl_2$–$DyCl_3$ (1.0 mol%) system.

Plateau No.	Potential vs Dy^{3+}/Dy, E/V[a)]					Coexisting phases
	1073 K	1098 K	1123 K	1148 K	1173 K	
(i)	0.165	0.164	0.151	0.150	0.150	$NiDy + Ni_2Dy$
(ii)	0.271	0.268	0.274	0.260	0.265	$Ni_2Dy + Ni_3Dy$
(iii)	0.502	0.500	0.500	0.474	0.476	$Ni_3Dy + Ni_5Dy$
(iv)	0.656	0.667	0.683	0.674	0.663	$Ni_5Dy + Ni$

a) The Dy^{3+}/Dy potentials were 0.391, 0.377, 0.360, 0.359, and 0.344 V vs. Ca^{2+}/Ca at 1073, 1098, 1123, 1148, and 1173 K, respectively.

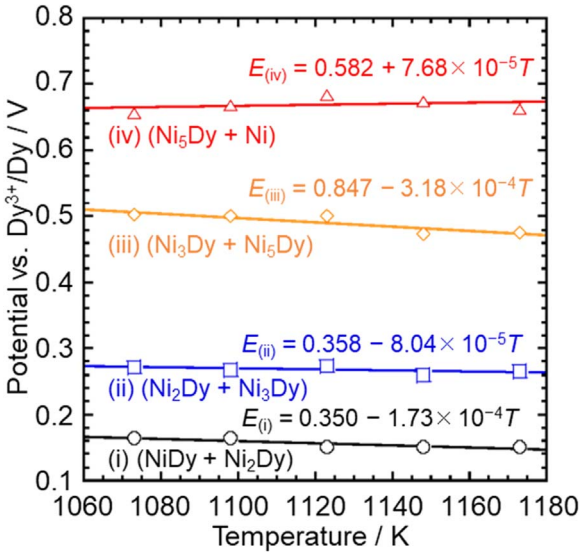

Figure 4. Temperature dependence of coexisting phase potentials for various Ni–Dy intermetallic compounds.

$$\Delta\bar{G}_{Dy} = -3FE \quad [5]$$

and

$$a_{Dy} = \exp\left(\Delta\bar{G}_{Dy}/RT\right) \quad [6]$$

where F is the Faraday constant and R is the gas constant. Next, using pure solid Ni as the standard state, the Ni activities (a_{Ni}) in the Ni–Dy intermetallic compounds were calculated using the Gibbs-Duhem equation:

$$\ln a_{Ni} = -\int_{X_{Ni}=1}^{X_{Ni}} \frac{X_{Dy}}{X_{Ni}} d\ln a_{Dy} \quad [7]$$

where X is the mole fraction of the component represented. According to the phase diagram,[37] all solid phases in this system are line compounds having negligible solid solution ranges. Thus, a_{Ni} for the (Ni_5Dy + Ni) state was considered as unity in this system. Then, the relative partial molar Gibbs energies of Ni ($\Delta\bar{G}_{Ni}$) were acquired using the equation:

$$\Delta\bar{G}_{Ni} = RT \ln a_{Ni} \quad [8]$$

The calculated $\Delta\bar{G}_{Dy}$ and $\Delta\bar{G}_{Ni}$ values are plotted in Fig. 5 and the regression equations are summarized in Table II. By substituting $\Delta\bar{G}_{Dy}$ and $\Delta\bar{G}_{Ni}$ into the Gibbs-Helmholtz equation,

$$\Delta\bar{G}_i = \Delta\bar{H}_i - \Delta\bar{S}_i \times T, \quad [9]$$

the relative partial molar enthalpies and entropies of Dy ($\Delta\bar{H}_{Dy}$ and $\Delta\bar{S}_{Dy}$) and Ni ($\Delta\bar{H}_{Ni}$ and $\Delta\bar{S}_{Ni}$) were calculated and the results are listed in Table III. In the enthalpy calculations, the entropy was assumed to be independent of temperature. The standard Gibbs energies of formation for Ni–Dy intermetallic compounds per mol·atom ($\Delta G^{\circ}_{f(Ni-Dy)}$) were calculated from $\Delta\bar{G}_{Dy}$ and $\Delta\bar{G}_{Ni}$ using the following equation:

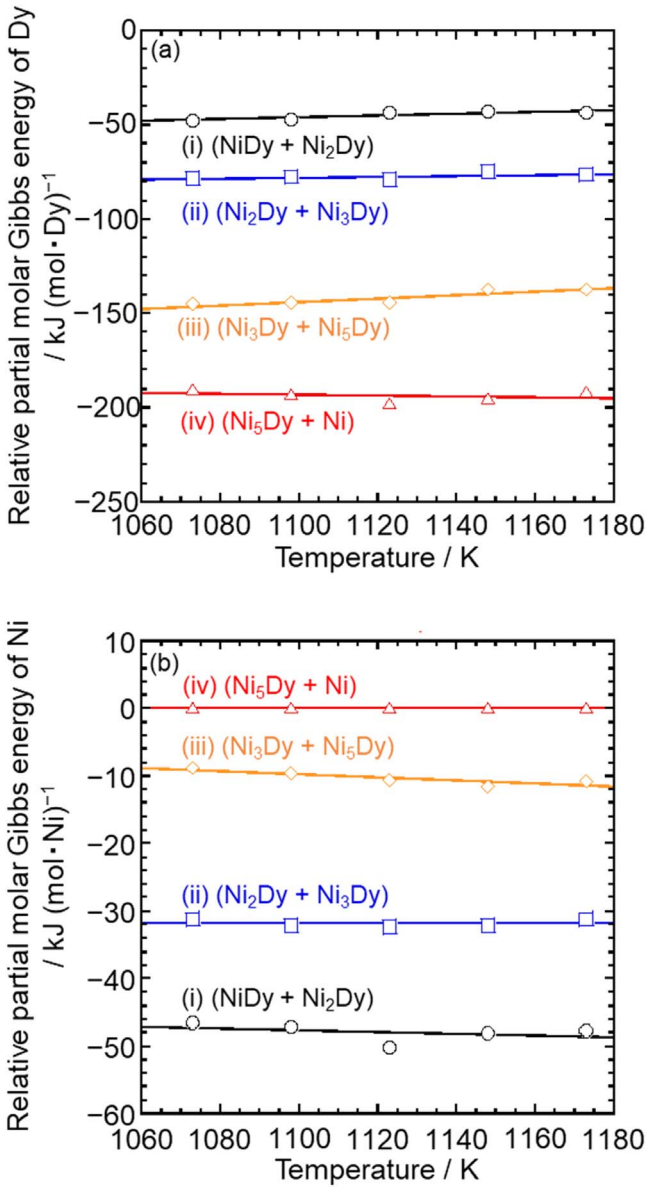

Figure 5. Temperature dependence of relative partial molar Gibbs energies of (a) Dy and (b) Ni for various Ni–Dy coexisting phase states.

Table II. Equations of the regression lines for the temperature dependence of relative partial molar Gibbs energies of Dy and Ni for Ni–Dy intermetallic compounds with coexisting phase states.

Coexisting phase	$\Delta\bar{G}_{Dy}$/J (mol·Dy)$^{-1}$	$\Delta\bar{G}_{Ni}$/J (mol·Ni)$^{-1}$
$NiDy + Ni_2Dy$	$-1.01 \times 10^5 + 5.00 \times 10\,T$	$-3.31 \times 10^4 - 1.33 \times 10\,T$
$Ni_2Dy + Ni_3Dy$	$-1.04 \times 10^5 + 2.33 \times 10\,T$	$-3.19 \times 10^4 + 6.95 \times 10^{-2}T$
$Ni_3Dy + Ni_5Dy$	$-2.45 \times 10^5 + 9.20 \times 10\,T$	$1.53 \times 10^4 - 2.29 \times 10\,T$
$Ni_5Dy + Ni$	$-1.69 \times 10^5 - 2.22 \times 10\,T$	0[a]

a) From the approximation that the activity of solid Ni is unity at all temperatures.

Table III. Relative partial molar enthalpies and entropies of Dy ($\Delta\bar{H}_{Dy}$ and $\Delta\bar{S}_{Dy}$) and Ni ($\Delta\bar{H}_{Ni}$ and $\Delta\bar{S}_{Ni}$) for Ni–Dy intermetallic compounds with coexisting phase states.

Coexisting phase	$\Delta\bar{H}_{Dy}$/kJ (mol·Dy)$^{-1}$	$\Delta\bar{H}_{Ni}$/kJ (mol·Ni)$^{-1}$	$\Delta\bar{S}_{Dy}$/J (mol·Dy)$^{-1}$ K^{-1}	$\Delta\bar{S}_{Ni}$/J (mol·Ni)$^{-1}$ K^{-1}
$NiDy + Ni_2Dy$	−101	−33.1	−50.0	13.3
$Ni_2Dy + Ni_3Dy$	−104	−31.9	−23.3	−0.0695
$Ni_3Dy + Ni_5Dy$	−245	15.3	−92.0	22.9
$Ni_5Dy + Ni$	−169	0	22.2	0

Table IV. Standard Gibbs energies of formation for Ni–Dy intermetallic compounds per mole atom.

Phase	ΔG_f°/J (mol·atom)$^{-1}$
NiDy	$-6.71 \times 10^4 + 1.84 \times 10\,T$
Ni_2Dy	$-5.58 \times 10^4 + 7.80\,T$
Ni_3Dy	$-4.98 \times 10^4 + 5.87\,T$
Ni_5Dy	$-2.81 \times 10^4 - 3.71\,T$

$$\Delta G^\circ_{f(Ni-Dy)} = X_{Dy} \times \Delta\bar{G}_{Dy} + X_{Ni} \times \Delta\bar{G}_{Ni} \quad [10]$$

The calculated results are shown in Table IV and plotted as black broken lines in Fig. 6 for comparison with the CALPHAD values reported by Li et al. (red broken lines).[33] Although the experimental temperatures are different (663–773 K), values reported by Konishi et al. (blue broken lines)[32] were also plotted. In Fig. 6, the solid lines indicate the experimental temperature range. The results obtained in this study were close to the two sets of reported values in the experimental temperature range of 1073–1173 K. However, they were slightly more negative than the CALPHAD values and slightly more positive than the experimental values of Konishi et al.

Finally, using the Gibbs-Helmholtz Eq. 9, the standard enthalpies and entropies of formation for Ni–Dy intermetallic compounds were calculated and are listed in Table V. For comparison, the standard enthalpies of formation reported by CALPHAD and calorimetry,[33,35,36] and the standard entropies of formation reported by CALPHAD are also listed. For the NiDy intermetallic compound, ΔH_f° of this study is more negative than the CALPHAD and calorimetry values. Also, ΔS_f° is more negative than the CALPHAD value. The ambiguity and difficulty in determining the potential plateau (i) in Fig. 3. might be one possible reason to cause this deviation. Since the potential shift to the plateau (i) could not be clearly observed, there may be slight inaccuracy in determining the start of the plateau (i). This small deviation may have caused the 16 J (mol·atom)$^{-1}$ K^{-1} difference in $\Delta S^\circ_{f(NiDy)}$, which would make $\Delta H^\circ_{f(NiDy)}$ more negative than the CALPHAD and calorimetry values. For the Ni_2Dy intermetallic compound, ΔH_f° and ΔS_f° of this study are almost the same as the CALPHAD values. However, the calorimetry value of ΔH_f° is more positive than both our value and the CALPHAD value. Nevertheless, the difference is smaller than that for the NiDy, which is likely due to the more accurate determination of the potential plateau (ii) than that of the plateau (i). For the Ni_3Dy intermetallic compound, both ΔH_f° and ΔS_f° are close to the CALPHAD values. Here, no calorimetry value has been reported for Ni_3Dy. As for the Ni_5Dy intermetallic compound, ΔH_f° is close to all the reported values. However, ΔS_f° of this study, 3.71 J (mol·atom)$^{-1}$ K^{-1}, is more positive than the CALPHAD value, −3.75 J (mol·atom)$^{-1}$ K^{-1}.

In this calculation, all our ΔH_f° values are more negative than calorimetry values. Since calorimetry is a method of directly detecting thermal variables, it should have higher accuracy than extrapolating ΔG_f° using ΔS_f°. In this study, the experiment temperature range was 100 K, which might not be wide enough. Thus, a wider experimental temperature should be tested for a more reliable determination.

Table V. Standard enthalpies and entropies of formation for Ni–Dy intermetallic compounds.

Phase	ΔH_f°/kJ (mol·atom)$^{-1}$				ΔS_f°/J (mol·atom)$^{-1}$ K^{-1}	
	This study	Li et al.[33] (CALPHAD)	Schott et al.[35] (Calorimetry)	Guo et al.[36] (Calorimetry)	This study	Li et al.[33] (CALPHAD)
NiDy	−67.1	−44.8	−33.4 ± 1.9	−35.2 ± 1.5	−18.4	−2.60
Ni_2Dy	−55.8	−50.7	−32.6 ± 1.8	—	−7.80	−7.82
Ni_3Dy	−49.8	−44.3	—	—	−5.87	−7.17
Ni_5Dy	−28.1	−32.1	−25.1 ± 0.9	−27.4 ± 0.7	3.71	−3.75

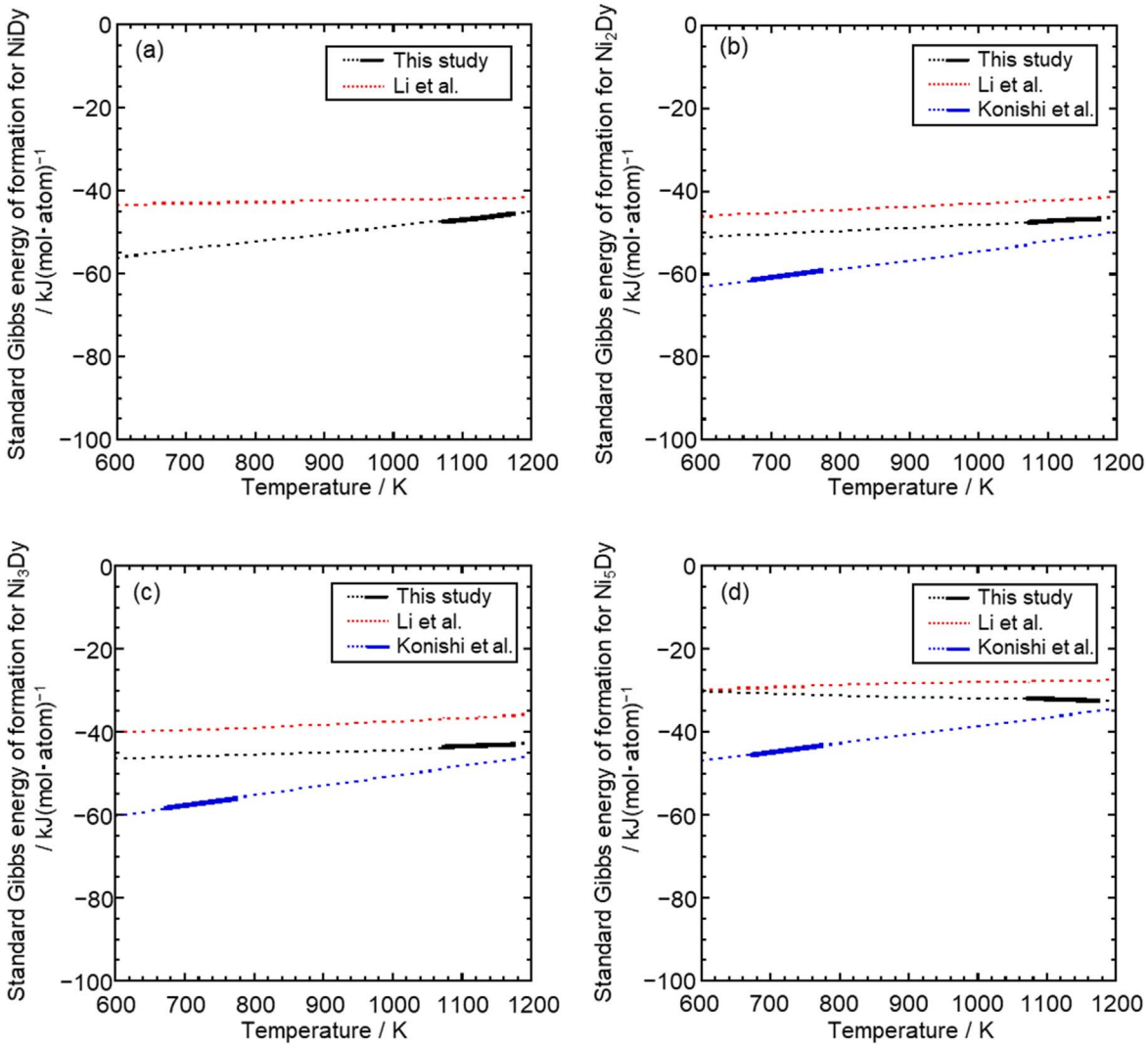

Figure 6. Calculated standard Gibbs energies of formation for (a) NiDy, (b) Ni_2Dy, (c) Ni_3Dy, and (d) Ni_5Dy based on experimental measurements[32] and the CALPHAD technique.[33] The solid line indicates the experimental temperature range.

Conclusions

The temperature dependence of the coexisting phase potentials for (NiDy + Ni_2Dy), (Ni_2Dy + Ni_3Dy), (Ni_3Dy + Ni_5Dy), and (Ni_5Dy + Ni) was investigated in the molten $CaCl_2$ containing 1.0 mol% $DyCl_3$ at 1073–1173 K. The relative partial molar thermodynamic properties and activities of Dy and Ni were calculated from the coexisting phase potentials. The values of $\Delta\bar{G}_{Dy}$ and $\Delta\bar{G}_{Ni}$ were used to calculate $\Delta G^{\circ}_{f(Ni-Dy)}$ for the NiDy, Ni_2Dy, Ni_3Dy, and Ni_5Dy intermetallic compounds. The obtained $\Delta G^{\circ}_{f(Ni-Dy)}$ values were compared, they showed good agreement with the reported values by CALPHAD and other experimental values between 1073 and 1173 K. Both $\Delta H^{\circ}_{f(Ni-Dy)}$ and $\Delta S^{\circ}_{f(Ni-Dy)}$ were compared with CALPHAD values and the slight differences may be due to inaccuracy in the potential determinations.

Acknowledgments

This work was partly supported by a Grant-in-Aid for Japan Society for the Promotion of Science (JSPS) Fellows grant number 19J20301.

ORCID

Hang Hua https://orcid.org/0000-0003-0010-5155
Kouji Yasuda https://orcid.org/0000-0001-5656-5359
Toshiyuki Nohira https://orcid.org/0000-0002-4053-554X

References

1. J. J. Croat, J. F. Herbst, R. W. Lee, and F. E. Pinkerton, *J. Appl. Phys.*, **55**, 2078 (1984).
2. M. Sagawa, S. Hirosawa, H. Yamamoto, S. Fujimura, and Y. Matsuura, *Jpn. J. Appl. Phys.*, **26**, 785 (1987).
3. R. Nakayama, T. Takeshita, M. Itakura, N. Kuwano, and K. Oki, *J. Appl. Phys.*, **70**, 3770 (1991).
4. R. E. Cech, *J. Metals*, **26**, 32 (1974).
5. J. J. Rhyne and S. Legvold, *Phys. Rev.*, **138**, A507 (1965).
6. K. H. J. Buschow, P. C. P. Bouten, and A. R. Miedema, *Rep. Prog. Phys.*, **45**, 937 (1982).
7. P. H. L. Notten and P. Hokkeling, *J. Electrochem. Soc.*, **138**, 1877 (1991).
8. G. Jin and H. Li, *J. Phys. Chem. Solids*, **62**, 2055 (2001).
9. J. Greeley, I. E. L. Stephens, A. S. Bondarenko, T. P. Johansson, H. A. Hansen, T. F. Jaramillo, J. Rossmeisl, I. Chorkendorff, and J. K. Nørskov, *Nat. Chem.*, **1**, 552 (2009).
10. D. Zubenko, S. Singh, and B. A. Rosen, *Appl. Catal., B*, **209**, 711 (2017).
11. N. Jones, *Nature*, **472**, 22 (2011).
12. J. M. D. Coey, *J. Magn. Magn. Mater.*, **248**, 441 (2002).
13. Y. Seo and S. Morimoto, *Resour. Policy*, **39**, 15 (2014).
14. A. Lukowiak, L. Zur, R. Tomala, T. N. LamTran, A. Bouajaj, W. Strek, G. C. Righini, M. Wickleder, and M. Ferrari, *Ceram. Int.*, **46**, 26247 (2020).
15. O. Takeda and T. H. Okabe, *Metall. Mater. Trans. E*, **1**, 160 (2014).
16. G. Adachi, K. Murase, K. Shinozaki, and K. Machida, *Chem. Lett.*, **21**, 511 (1992).
17. T. Uda, K. T. Jacob, and M. Hirasawa, *Science*, **289**, 2326 (2000).
18. T. Uda, *Mater. Trans.*, **43**, 55 (2002).
19. T. H. Okabe, O. Takeda, K. Fukuda, and Y. Umetsu, *Mater. Trans.*, **44**, 798 (2003).
20. T. Saito, H. Sato, S. Ozawa, J. Yu, and T. Motegi, *J. Alloy. Compd.*, **353**, 189 (2003).
21. O. Takeda, T. H. Okabe, and Y. Umetsu, *J. Alloy. Compd.*, **379**, 305 (2004).

22. M. Itoh, M. Masuda, S. Suzuki, and K.-I. Machida, *J. Alloy. Compd.*, **374**, 393 (2004).
23. Y. Xu, L. S. Chumbley, and F. C. Laabs, *J. Mater. Res.*, **15**, 2296 (2000).
24. O. Takeda, K. Nakano, and Y. Sato, *Mater. Trans.*, **55**, 334 (2014).
25. T. Akahori, Y. Miyamoto, T. Saeki, M. Okamoto, and T. H. Okabe, *J. Alloy. Compd.*, **703**, 337 (2017).
26. S. Shirayama and T. H. Okabe, *Metall. Mater. Trans. B*, **49**, 1067 (2018).
27. T. Nohira, S. Kobayashi, K. Kondo, K. Yasuda, R. Hagiwara, T. Oishi, and H. Konishi, *ECS Trans.*, **50**, 473 (2012).
28. K. Yasuda, K. Kondo, S. Kobayashi, T. Nohira, and R. Hagiwara, *J. Electrochem. Soc.*, **163**, D140 (2016).
29. H. Konishi, H. Ono, T. Nohira, and T. Oishi, *ECS Trans.*, **50**, 463 (2012).
30. H. Hua, K. Yasuda, H. Konishi, and T. Nohira, *J. Electrochem. Soc.*, **167**, 142504 (2020).
31. H. Hua, K. Yasuda, H. Konishi, and T. Nohira, *J. Electrochem. Soc.*, **168**, 032506 (2021).
32. H. Konishi, T. Nishikiori, T. Nohira, and Y. Ito, *Electrochim. Acta*, **48**, 1403 (2003).
33. M. Li and W. Han, *Calphad*, **33**, 517 (2009).
34. K. Nassau, *PhD Thesis*, University of Pittsburgh (1959), University Microfilms, Mic.59-6551.
35. J. Schott and F. Sommer, *J. Less-Common Met.*, **119**, 307 (1986).
36. Q. Guo and O. J. Kleppa, *Metall. Mater. Trans. B*, **27B**, 417 (1996).
37. H. Okamoto, *J. Phase Equilib. Diffus.*, **35**, 105 (2014).